



Title	Experimental Study of Brittle Fracture with Plastic Strain at Cruciform Butt Joints (Report III) : Effect of bi-axial loading condition(Mechanics, Strength & Structure Design)
Author(s)	Sakino, Yoshihiro; Kamura, Hisaya; Horikawa, Kohsuke
Citation	Transactions of JWRI. 2000, 29(1), p. 97-104
Version Type	VoR
URL	<a href="https://doi.org/10.18910/4916">https://doi.org/10.18910/4916</a>
rights	
Note	

*The University of Osaka Institutional Knowledge Archive : OUKA*

<https://ir.library.osaka-u.ac.jp/>

The University of Osaka

# Experimental Study of Brittle Fracture with Plastic Strain at Cruciform Butt Joints<sup>†</sup> (Report III)

— Effect of bi-axial loading condition —

Yoshihiro SAKINO\*, Hisaya KAMURA\*\* and Kohsuke HORIKAWA\*\*\*

## Abstract

*In The Great Hanshin-Awaji Earthquake Disaster, brittle fractures with plastic strain were observed in beam-column connections of steel building frames. It is considered that the mechanical properties of weld metal, especially the ductility, affected the fractures.*

*In Report I, we described monotonic loading test results using cruciform butt specimens welded by three types of welding consumable. We examined the effect of mechanical properties of weld metal on fractures under monotonic loading. And in Report II, we described test results to examine the effect of cyclic loading like the earthquake.*

*In this Report III, we describe monotonic bi-axial loading test results under two types of bi-axial loading condition using the cruciform butt specimens. The purpose of this paper is to examine the effect of bi-axial loading condition on fractures.*

*The main results are summarized as follows. 1) The effects of the bi-axial loading condition on the elongation capacity and the fracture-surface appearance are small compared to the ductility of the material and temperature of the specimen.*

*And by this experiment, the following considerations about the elongation capacity and the fracture-surface appearance become more reliable. 2) The ductility of weld metal greatly affects the elongation capacity regardless of other conditions. In the case of the cruciform butt joints with brittle weld metal, the temperature of the specimen also greatly affects the elongation capacity. 3) The fracture-surface appearance of the specimen is mainly affected by the temperature of the specimen that substituted for high strain rates.*

**KEY WORDS:** (Damage due to Earthquake) (Steel Structures) (Welded Joints)(Cruciform Joints)  
(Charpy Absorbed Energy) (Brittle Fracture)(Bi-axial Loading)

## 1. Introduction

In The Great Hanshin-Awaji Earthquake, fractures were observed in beam-column connections of steel building frames. These parts have the largest load, so that they become the most important part of the frame. These fractures are divided into two types, either due to insufficient strength or to brittle fracture. The former type was found in comparatively older buildings welded according to the old design standards. However the latter type of damage occurred in connections welded according to the present design standards. It was ascertained by marks of local buckling, peeling of paint or mill scale and Luders's lines, that these fractured after plastic deformations. In this context, these are regarded

as "general yield brittle fractures", because they fractured at stress concentration points or discontinuous points of shape after absorption of seismic energy. More studies are needed about the influencing factors and about the energy absorption capacity of general yield brittle fracture.<sup>1-5)</sup>

Typical modes of brittle fracture in beam-column connections are divided as follows.

(Mode-A) Brittle fractures in base metal at beam-flanges, starting from the toe of the weld access hole (scallop) in the web.

(Mode-B) Brittle fractures in base metal, heat-affected zone or weld metal of welded connections, starting from the backing strip or the end tab.

It is considered that the mechanical properties of base metal and the detail of the scallop, the backing strip

<sup>†</sup> Received on June 12, 2000

\* Research Associate

\*\* NKK CORPORATION

\*\*\* Professor

Transactions of JWRI is published by Joining and Welding Research Institute of Osaka University, Ibaraki, Osaka 567-0047, Japan.

and the end tab have substantial effects on the Mode-A and Mode-B forms of fracture. It was reported that the plastic deformation-capacity of the beam to column connections became large following improvement of the detail of the scallop.<sup>6)</sup>

As well as the above influencing factors, it can be considered that the mechanical properties of weld metal, especially the ductility of weld metal, have substantial effects in Mode-B. (In this paper, the mechanical properties represent the absolute values of the elongation in the tensile test and the absorbed energy in Charpy impact test.) In the Report I<sup>7)</sup>, we described monotonic bi-axial loading test results using cruciform butt specimens welded by three types of welding consumable. The purpose of the Report I was to clarify the effect of the mechanical properties of weld metal on fractures under monotonic loading. In Report II<sup>8)</sup>, we described cyclic bi-axial loading test results for cruciform butt specimens that are the same as Report I. The purpose of this paper was to examine the effect of cyclic loading and to clarify the difference between monotonic and cyclic loading on fractures. Because the structures endure cyclic loading during an earthquake and it was necessary to clarify the effect of cyclic loading.

In this Report III, we describe monotonic bi-axial loading test results under two types of bi-axial loading condition using cruciform butt specimens that are the same as Report I and II. The purpose of this paper is to examine the effect of the bi-axial loading condition on fractures.

## 2. Experimental Details

### 2.1 Shape of the specimen

As shown in Fig. 1, the shape of the specimen for the bi-axial loading test is the same in the Report I and II. It is modeled on a cruciform joint by taking out the part of the beam-flange to column-flange connection. In the specimen, butt welds are at the crossover point of

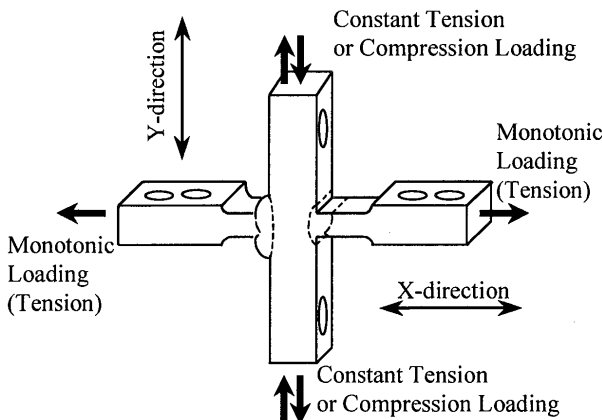


Fig. 1 A conception shape of cruciform butt specimen and Loading Condition

flanges which appear to be the most critical zone for fracture. Single bevel grooves with full penetration were used to make the cruciform butt weld. After welding, excess weld metal is removed and the width of the weld part is narrowed from 40mm to 30mm and an artificial notch is added in the thickness direction as an initial defect by the electric wire-cut method as the same in the Report I and II. But the depth of an artificial notch is 3mm and it is larger than that in the specimens in the Report I and II (2mm). The detail of the weld zone is shown in Fig. 2.

### 2.2 Experimental parameters

Besides the bi-axial loading condition, the ductility of weld metal and temperature of the specimen are varied in this experiment.

#### 2.2.1 Biaxial loading condition

Two types of the bi-axial loading condition were used. One was the tension stress in the Y-direction and another was the compression stress in the Y-direction. As shown in Fig. 1, first the specimen was subjected to tensile or compression load (60% of yield strength of base metal) in the Y-direction and the load kept constant, then continuously loaded in the X-direction till it fractures. In general condition, column-flanges are subjected compression load by dead load (the weight of the building), so the stress in the Y-direction is compression. The tension stress condition in the Y-direction corresponds to a beam-column connection subjected to the vertical vibration or the tensile force by the overturning moment during earthquake.

In this paper, the specimen that received tensile loading in the Y-direction is named "the tensile specimen" and the specimen that received compression loading in the Y-direction is named "the compression specimen".

A bi-axial fatigue machine was used in the experiment. This machine has four jacks and can load in two directions at the same time. The displacements

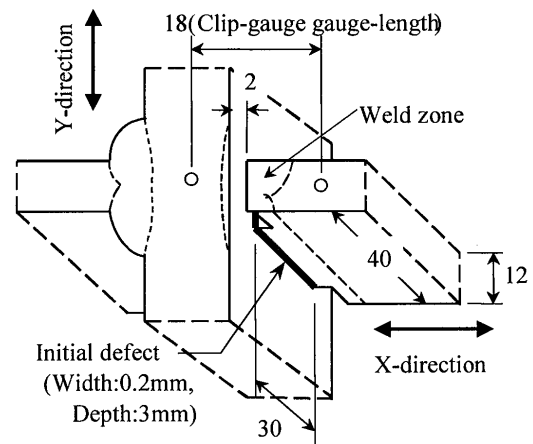


Fig. 2 Detail of weld zone and measuring points

between the 18mm gauge-lengths, shown in Fig. 2, were measured by two clip-gauges fixed to both sides of the specimen.

### 2.2.2 Ductility of Weld metals

Two types of weld metal were used in this experiment. The NY-series specimens were welded by CO<sub>2</sub> shielded gas wire (JIS Z 3312 YGW11) and the NS-series specimens were welded by self-shielded wire (JIS Z 3313 YFW-S50GX). The minimum value of Charpy observed energy at 0°C ( $vE_0$ ) is provided for YGW11 as 47J, but not provided for YFW-S50GX in JIS. (JIS: Japanese Industrial Standard)

Table 1 and Fig. 3 show tensile test results for each weld metal. Table 2 and Fig. 4, 5 show Charpy impact test results for each weld metal. Fig. 6 shows the comparisons of energy transition curves of all weld metal. JIS Z 2201 No.14 test pieces (diameter:10mm) were used for the tensile test and JIS Z 2202 No.4 test pieces for the Charpy impact test. All test pieces of weld metal were cut from deposited parts. Energy and fracture transition curves by Charpy impact test are fitted

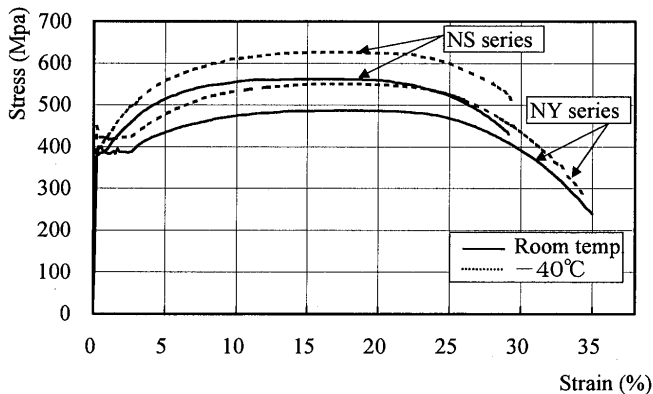


Fig. 3 Stress-strain curves of weld metal by tensile test

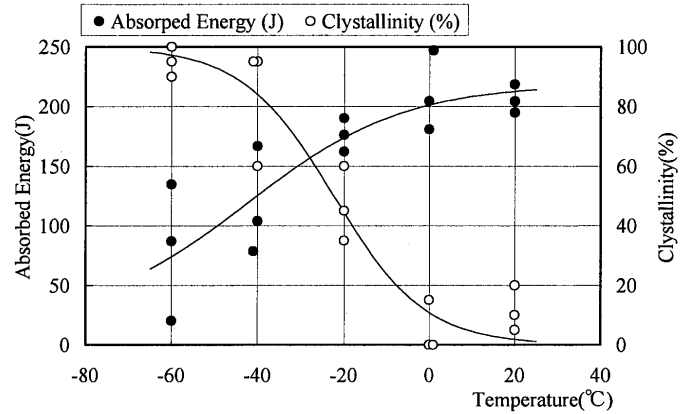


Fig. 4 Energy and fracture transition curves by Charpy impact test (NY-series)

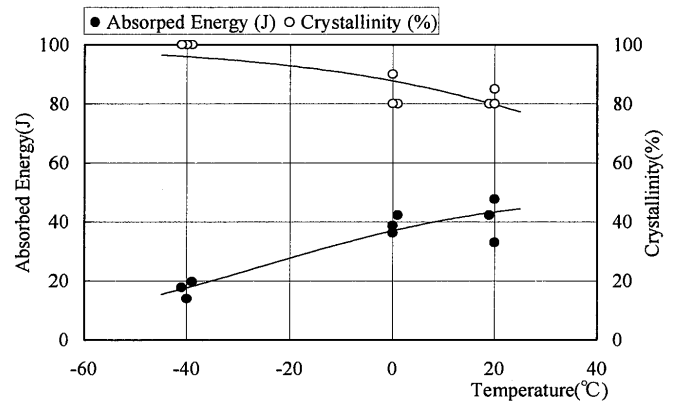


Fig. 5 Energy and fracture transition curves by Charpy impact test (NS-series)

Table 1 Results of tensile test (weld metal and base metal)

	Weld metal								Base metal*							
	-40°C				Room temp.				Column-flange				Beam-flange			
	$\sigma_y$ (MPa)	$\sigma_u$ (MPa)	$\epsilon_f$ (%)	$\phi$ (%)	$\sigma_y$ (MPa)	$\sigma_u$ (MPa)	$\epsilon_f$ (%)	$\phi$ (%)	$\sigma_y$ (MPa)	$\sigma_u$ (MPa)	$\epsilon_f$ (%)	$\phi$ (%)	$\sigma_y$ (MPa)	$\sigma_u$ (MPa)	$\epsilon_f$ (%)	$\phi$ (%)
NY-series	421	550	33	73	396	487	34	74	326*	490*	24*	-	415*	539*	28*	-
NS-series	407	638	30	51	380	562	29	56	363*	522*	23*	-	402*	525*	27*	-

$\sigma_y$ : Yield stress,  $\sigma_u$ : Tensile strength,  $\delta$ : Total elongation,  $\phi$ : Reduction of area \*: from mill sheet

Table 2 Result of Charpy impact test

	Weld metal								
	Absorbed energy(J)							Transition temp. (°C)	
	-60°C	-40°C	-20°C	0°C	+20°C	+40°C	+60°C	$vT_{RE}$	$vT_{RS50}$
NY-series	81	116	176	211	206	-	-	-42.2	-22.4
NS-series	-	17	-	39	41	-	-	>+20	>+20

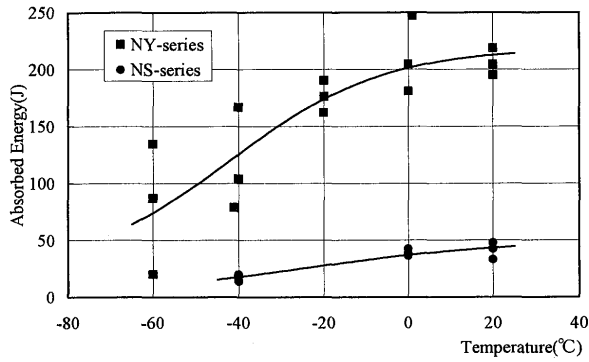


Fig. 6 Comparison of energy transition curves

The Charpy absorbed energies of the NY-series are over 100J, either at room temperature or  $-40^{\circ}\text{C}$ . The NS-series are less than 50J in all ranges from  $-40^{\circ}\text{C}$  to  $+20^{\circ}\text{C}$ , but clear of the value of 27J at  $0^{\circ}\text{C}$  that is required for steels for welded building structures in JIS as a minimum. The energy transition temperature  $vT_{RE}$  and the fracture-surface transition temperature  $vT_{RS50}$  of the NY-series are under  $-20^{\circ}\text{C}$ . On the other hand, the crystallinity of the NS-series at  $+20^{\circ}\text{C}$  is about 80%, so it seems that  $vT_{RE}$  and  $vT_{RS50}$  of the NS-series are very high (at least more over  $+20^{\circ}\text{C}$ ). So the Charpy impact test results suggest that the weld metal of the NY-series is high ductility weld metal

(ductile weld metal) and the NS-series has low ductility weld metal (brittle weld metal) compared to the NY-series.

### 2.2.3 Temperature of specimens

It is generally known that the strain rate affects the deformation and fracture of steel. In fact, it is considered that the high strain rate is one of the substantial causes of damage in The Great Hanshin-Awaji Earthquake. Because the fracture toughness of steel declines with increasing strain rate, in the same way, fracture toughness of steel also declines at low test-temperatures. As the parameter to evaluate the effect of the strain rate and low test temperature equivalently, a strain rate-temperature parameter (R) is proposed.<sup>10, 11)</sup> It becomes possible to substitute for high strain rates in static tests at low temperature by using this R-parameter.

Experiments were done not only at room temperature but also  $-40^{\circ}\text{C}$ . Static experiments at  $-40^{\circ}\text{C}$  can approximately represent the loading condition in The Great Hanshin-Awaji Earthquake.

During the low temperature experiment the specimen was cooled by ethyl alcohol and liquid nitrogen kept at  $-40\pm 2^{\circ}\text{C}$ . Temperature was measured by two points of thermocouples (C-C type) fixed on the specimen.

Table 3 Results of bi-axial monotonic test

Specimen No.	Temp. ( $^{\circ}\text{C}$ )	Y-direction Loading	Load (kN)		Disp. of clip gauge (mm)		Fracture surface (Crystallinity)
			Max.	Fracture	Max.	Fracture	
NYRT-1	+23	Tension	216.4	212.1	2.03	Max.	Ductile (10%)
NYRT-2	+21	Tension	195.8	195.3	1.36	1.58	Ductile(0%)
NYRC-1	+20	Compression	192.0	191.6	1.29	1.50	Ductile(0%)
NYRC-2	+13	Compression	205.8	205.4	1.41	1.53	Ductile(0%)
NYLT-1	-40	Tension	215.0	Max.	0.92	Max.	Brittle(95%)
NYLT-2	-40	Tension	223.2	222.9	1.62	1.70	Brittle(85%)
NYLT-3	-40	Tension	244.2	244.3	2.01	2.16	D $\rightarrow$ B(70%)
NYLC-1	-40	Compression	218.8	218.6	1.26	1.31	Brittle(85%)
NYLC-2	-40	Compression	210.8	Max.	1.00	Max.	D $\rightarrow$ B(65%)
NSRT-1	+28	Tension	189.0	188.8	0.94	1.07	Ductile (25%)
NSRT-2	+28	Tension	182.2	Max.	1.22	Max.	D $\rightarrow$ B(65%)
NSRC-1	+28	Compression	181.8	181.1	1.41	1.44	Ductile(0%)
NSRC-2	+28	Compression	187.9	187.8	0.87	0.93	Brittle (75%)
NSLT-1	-40	Tension	188.5	Max.	0.68	Max.	Brittle(100%)
NSLT-2	-40	Tension	171.8	Max.	0.49	Max.	Brittle(100%)
NSLC-1	-40	Compression	179.6	Max.	0.40	Max.	Brittle(100%)
NSLC-2	-40	Compression	183.5	Max.	0.44	Max.	Brittle(100%)

D $\rightarrow$ B: Brittle fracture occurred after developing the ductile crack

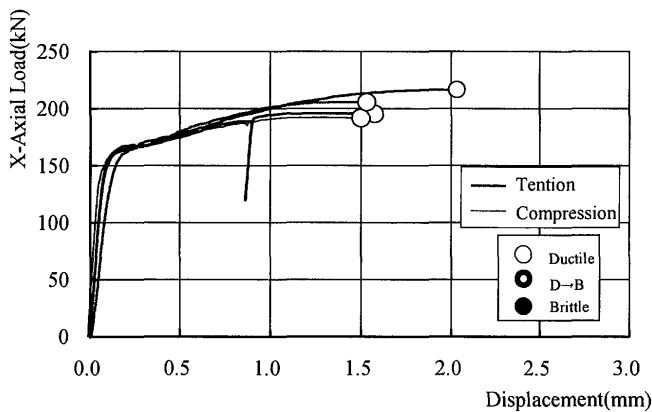


Fig.7 X-axial load - displacement relationship  
(NY-series, Room temperature)

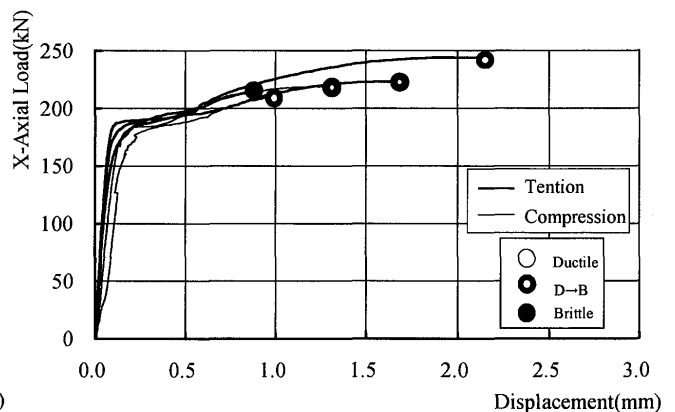


Fig.8 X-axial load - displacement relationship  
(NY-series, -40 °C)

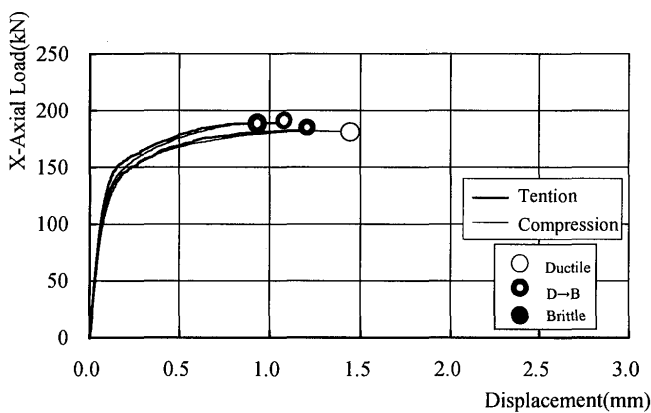


Fig.9 X-axial load - displacement relationship  
(NS-series, Room temperature)

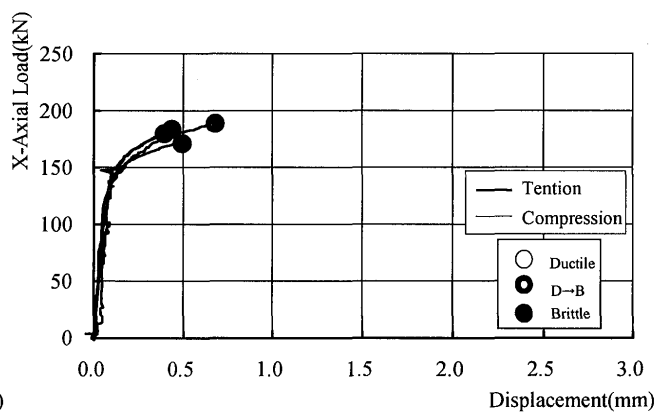


Fig.10 X-axial load - displacement relationship  
(NS-series, -40 °C)

### 3. Results and Discussion

Table 3 shows the results of the bi-axial tensile test. Load-displacement relationships of the NY-series and the NS-series at room temperature and -40°C are shown in Fig. 7 - Fig. 10. The displacement in these figures is the average of two clip-gauge readings.

All specimens fractured immediately after the maximum load. And as in Report I and II, three types of fracture-surface, ductile fracture-surface, brittle fracture-surface and intermingled fracture-surface were observed. In the intermingled fracture-surface specimens, it seems that the brittle fracture occurred after developing the ductile crack ( $D \Rightarrow B$ : ductile  $\Rightarrow$  brittle). In Fig.7 - Fig.10, symbol  $\circ$  means the ductile fracture-surface, symbol  $\bullet$  means the brittle fracture-surface and symbol  $\odot$  means the intermingled fracture-surface ( $D \Rightarrow B$ , area ratio of black in the symbol shows brittle fracture-surface ratio). In the specimens with a ductile fracture-surface, the crack runs at 45° to the Y-direction from the tip of the initial defect. But in the specimens with a brittle fracture-surface, the crack

runs at right-angles to the Y-direction from the tip of the initial defect. In this paper, fractures with equal to or more than 75% of the crystallinity are classified into "the brittle fracture", with equal to or less than 25% are classified into "the ductile fracture" and with from 30% to 70% are classified into "the intermingled fracture". Fig. 14 - Fig. 16 in Report I show the specimens that fractured with a ductile fracture-surface, with a brittle fracture-surface and with an intermingled fracture-surface.

#### 3.1 Effect of ductility of weld metal and temperature

In this section, the effect of the ductility of the weld metal and the temperature of the specimen on the elongation capacity and fracture-surface appearance are discussed. These are also discussed in Report I. As well as the bi-axial loading condition, the welding consumables and the depth of an artificial notch in the specimen are different from that in Report I. So these are reconsidered by the results of the NY-series and the NS-series and these results are compared to that in Report I.

### 3.1.1 Elongation capacity

The comparisons of the elongation capacity by the difference of the Charpy absorbed energy of the weld metals are shown in Fig. 11 and elongations in this figure are presented as the non-dimension value (that divided by the elongation of the ductile specimen (NY-series) at the same temperature and in the same loading condition in the Y-direction).

Regardless of temperature of the specimen and the loading condition in the Y-direction, the elongation capacity declines due to the reduction of the Charpy absorbed energy of the weld metal. In particular, the decline ratio at  $-40^{\circ}\text{C}$  is very large and the elongation capacities decline less than half.

The comparisons of the elongation capacity by the difference of temperature are shown in Fig. 12 and elongations in this figure are also presented as the non-dimension value (that divided by the elongation at room temperature with the same ductility and in the same loading condition in the Y-direction).

In the case of the specimens with brittle weld metal (NS-series), the elongation capacity declines due to the fall of temperature regardless of the loading condition in the Y-direction. The decline ratio is also large and elongation capacities decline by about half. In the case

of the specimens with ductile weld metal (NY-series), elongations are scattered but it seems that the effect of temperature of the specimen is not so large.

As described above, the ductility of weld metal greatly affects the elongation capacity regardless of other conditions. In case of the specimens with brittle weld metal, temperature of the specimen also affects the elongation capacity. These results are almost equal to those in the Y-series and the S-series discussed in Report I. So it seems that these considerations about the elongation capacity become more reliable by this experiment.

### 3.1.2 Fracture-surface appearance

The comparisons of the crystallinity of the fracture-surface by the difference of the Charpy absorbed energy are shown in Fig. 13. The crystallinity of the fracture-surface of the specimens become large due to the reduction of the Charpy absorbed energy of weld metal. But the increase ratios of crystallinity are not so large compared with the great difference of the Charpy absorbed energy (from 200J to 40J).

The comparisons of the crystallinity of the fracture-surface by the difference of temperature are shown in Fig. 14. The crystallinities of fracture

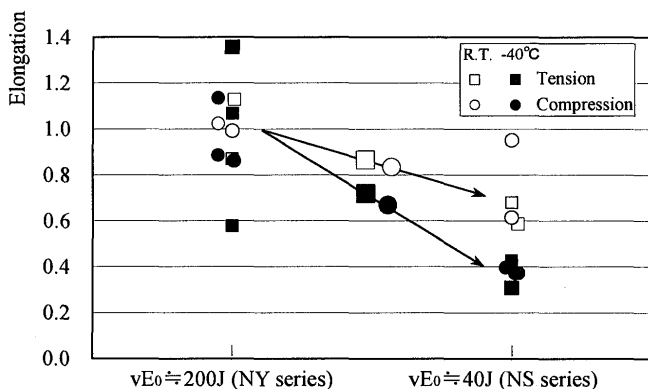


Fig. 11 Comparison by Charpy absorbed energy (Elongation)

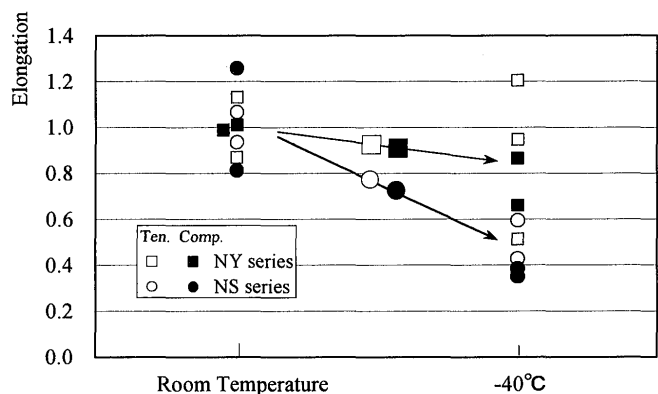


Fig. 12 Comparison by specimen temperature (Elongation)

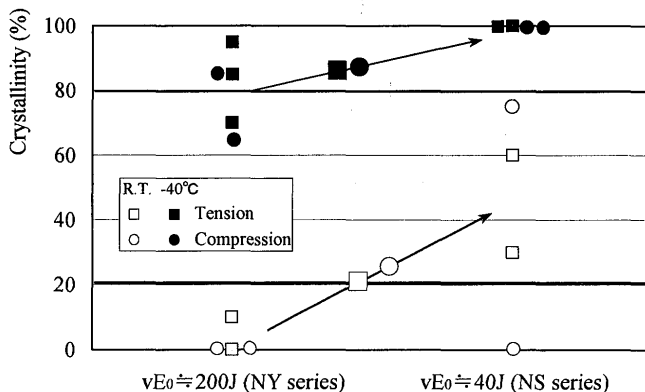


Fig. 13 Comparison by Charpy absorbed energy (Crystallinity)

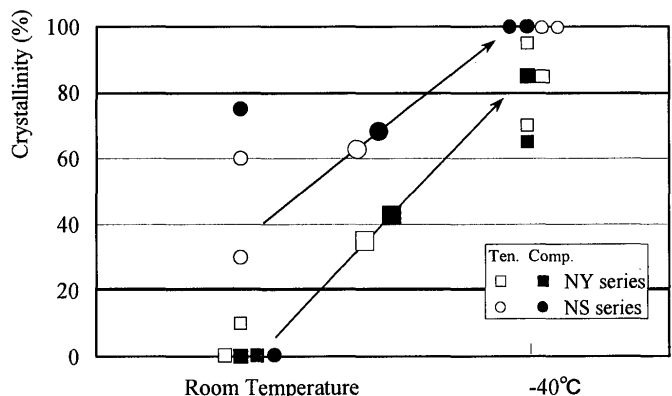


Fig. 14 Comparison by specimen temperature (Crystallinity)

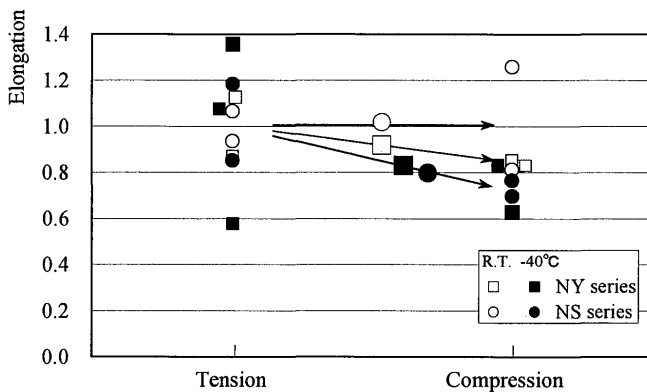


Fig. 15 Comparison by loading in Y-direction (Elongation)

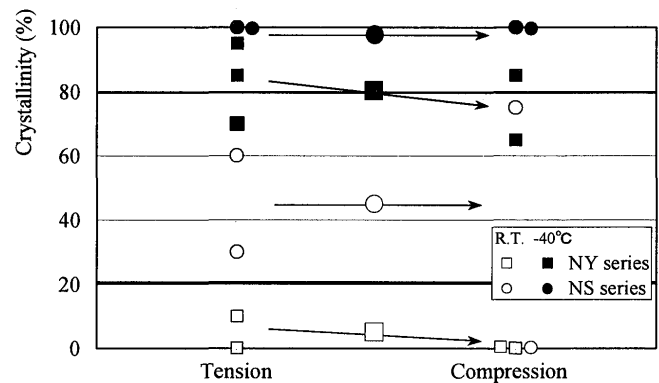


Fig. 16 Comparison by loading in Y-direction (Crystallinity)

-surfaces of the specimens become extremely large due to the fall of temperature regardless of the loading condition in the Y-direction and the ductility of weld metal. All specimens at  $-40^{\circ}\text{C}$  showed brittle fracture or the intermingled fracture where crystallinity is large.

As described above, the fracture-surface appearance of the specimens are mainly affected by the temperature of the specimen that substituted for high strain rates. The effect of the ductility of weld metal on the fracture-surface appearance of the specimen is small compared with the temperature of the specimen. These results are equal to those in the Y-series and the S-series discussed in Report I. So it seems that these considerations about the fracture-surface appearance also become more reliable by this experiment.

### 3.2 Effect of bi-axial loading condition

In this section, the bi-axial test results under tensile loading and compression loading in the Y-direction are compared.

#### 3.2.1 Elongation capacity

The comparisons of the elongation capacity for the differences in the loading conditions in the Y-direction are shown in Fig. 15. Elongations are presented as the non-dimension value (that divided by the elongation of the tensile specimen at the same temperature and with the same ductility).

Regardless of the ductility of weld metal, the elongation capacity declines due to changing from tension loading to compression loading in the Y-direction. At room temperature, elongations of compression specimens are approximately equal to or slightly smaller than those of the tension specimens. The experimental values of the tension specimens at  $-40^{\circ}\text{C}$  are very scattered. But elongation capacities of the compression specimens at  $-40^{\circ}\text{C}$  tend to be smaller than those of the tension specimens in this experiment. The decline rate of elongations at  $-40^{\circ}\text{C}$  is larger than that at room temperature. But the decline rate of

elongations caused by the difference in the loading condition in the Y-direction is much smaller than that caused by the difference of the ductility of the weld metal.

These results indicate that the effect of the bi-axial loading condition to the elongation capacity is small compared to the ductility of the material.

#### 3.2.2 Fracture-surface appearance

The comparisons of the crystallinity by the difference of the loading condition in the Y-direction are shown in Fig. 16.

Regardless of the ductility of the weld metal and the temperature of the specimen, crystallinities of fracture-surfaces of the specimens are almost the same in tension loading and compression loading in the Y-direction. All specimens at  $-40^{\circ}\text{C}$  showed brittle fracture or the intermingled fracture (crystallinity is large), and all specimens at room temperature showed ductile or the intermingled fracture (crystallinity is small).

These results indicate that the bi-axial loading conditions do not affect the fracture-surface appearance. So the fracture pattern mainly depends on temperature of the specimen that substituted for high strain rates.

### 4. Conclusions

In this study, cruciform butt specimens that had initial defects were welded using two types of welding consumable and tested under two type of bi-axial loading condition at room temperatures and  $-40^{\circ}\text{C}$  to examine the effect of the bi-axial loading condition on fractures.

The investigation results are summarized as follows.

- (1) The ductility of the weld metal greatly affects the elongation capacity regardless of other conditions. In the case of the cruciform butt joints with brittle weld metal, temperature of the specimen also



greatly affects the elongation capacity.

- (2) The fracture-surface appearance of the specimen is mainly affected by the temperature of the specimen that substituted for high strain rates.
- (3) The effects of the bi-axial loading conditions on the elongation capacity and the fracture-surface appearance are small compared to the ductility of the material and temperature of the specimen.

## Acknowledgments

The author would like to thank Mr. Y.NAKATSUJI and Mr. H.KAWAZU for his help during the experiments. This study was financially supported in part by the Grant-in-Aid for Encouragement Research (A) from the Ministry of Education, Science and Culture.

## Reference

- 1) M.TOYODA: How Steel Structures Fared in Japan's Great Earthquake, Welding Journal, American Welding Society, December (1995), pp.31-42
- 2) Committee on Steel Building Structures, The Kinki-Branch of The Architectural Institute of Japan (AIJ): Reconnaissance Report on Damages to Steel Building Structures Observed in the 1995 Hyogoken-Nanbu (Hanshin /Awaji) Earthquake, 1995(in Japanese)
- 3) Japanese Society of Steel Construction (JSSC): KOBE EARTHQUAKE DAMAGE TO STEEL MOMENT CONNECTIONS AND SUGGESTED IMPROVEMENT, JSSC Technical Report, No.39 (1997)
- 4) K.HORIKAWA and Y.SAKINO: Review of Damage in Welding Joints Caused by The Kobe Earthquake, Trans. of Welding Research Institute of Osaka University (JWRI), Vol.24 (1995), No.2, pp.1-10
- 5) K.HORIKAWA and Y.SAKINO: Damage due to Steel Structures Caused by the 1995 Kobe Earthquake, Structural Engineering International, J. Int. Ass. for Bridge and Structural Engineering (IABSE), Vol.6(1995), No.3, pp.182-183
- 6) Committee on Steel Building Structures, The Kinki-Branch of The Architectural Institute of Japan (AIJ): Full-Scale Test on Plastic Rotation Capacity of Steel Wide-Flange Beams Connected with Square Tube Columns, 1997 (in Japanese)
- 7) Y.SAKINO, K.HORIKAWA, H.KAWAZU and H. KAMURA: Experimental Study on Brittle Fractures with Plastic Strain at Cruciform Butt Joints (Report I ): Trans. of JWRI , Vol.26(1997),No.2, pp81-88
- 8) Y.SAKINO, K.HORIKAWA, H.KAWAZU and H. KAMURA: Experimental Study on Brittle Fractures with Plastic Strain at Cruciform Butt Joints (Report II): Trans. of JWRI , Vol.27(1998),No.1, pp97-104
- 9) F.NOgATA, J.MASAKI: New fitting curve for Charpy Absorbed Energy and fracture toughness data of steel: J. of the Japanese Soc. for Strength and Fracture of materials, Vol.17(1982)No.2, pp1-13 (in Japanese)
- 10) P.E.Bennett, G.M.Sinclair: Parameter representation of low-temperature yield behavior of body-centered cubic transition metals, Transaction of the ASME, (1966), 518-524
- 11) P.E.Bennett, G.M.Sinclair: An analysis of the time and temperature dependence of the upper yield point iron, Transaction of the ASME, J. Basic Eng., 33(1961), 557.
- 12) Committee on Accumulated Plastic Deformation, The Japan Welding Engineering Society : Strength and fracture toughness of welding connections in steel building under cyclic large deformation (Interim Report I , II , III ) , 1996.7(in Japanese)